Multiphoton quantum interference at a beam splitter and the approach to Heisenberg-limited interferometry

Richard Birrittella, Jihane Mimih, and Christopher C. Gerry
Department of Physics and Astronomy, Lehman College, The City University of New York, Bronx, New York 10468-1589, USA
(Received 1 August 2012; published 21 December 2012)

We study multiphoton quantum-interference effects at a beam splitter and its connection to the prospect of attaining interferometric phase-shift measurements with noise levels below the standard quantum limit. Specifically, we consider the mixing of the most classical states of light coherent states with the most nonclassical states of light number states at a 50 : 50 beam splitter. Multiphoton quantum-interference effects from mixing photon-number states of small photon numbers with coherent states of arbitrary amplitudes are dramatic even at the level of a single photon. For input vacuum and coherent states, the joint photon-number distribution after the beam splitter is unimodal, a product of Poisson distributions for each of the output modes but with the input of a single photon, the original distribution is symmetrically bifurcated into a bimodal distribution. With a two-photon-number state mixed with a coherent state, a trimodal distribution is obtained, etc. The obtained distributions are shown to be structured so as to be conducive for approaching Heisenberg-limited sensitivities in photon-number parity-based interferometry. We show that mixing a coherent state with even a single photon results in a significant reduction in noise over that of the shot-noise limit. Finally, based on the results of mixing coherent light with single photons, we consider the mixing coherent light with the squeezed vacuum and the squeezed one-photon states and find the latter yields higher sensitivity in phase-shift measurements for the same squeeze parameter owing to the absence of the vacuum state.

DOI: 10.1103/PhysRevA.86.063828 PACS number(s): 42.50.St, 42.50.Lc, 42.50.Ex, 06.20.Dk

I. INTRODUCTION

The familiar coherent states $|\alpha\rangle$ [1] are the most classical-like of all the pure states of a single-mode quantized electromagnetic field, and they represent the light produced by a phase-stabilized laser. They yield field-operator expectation values that behave like classical prescribed fields but with quantum fluctuations at the level of the vacuum. The corresponding Wigner function is Gaussian and positive everywhere in phase space, whereas, its corresponding P function [1,2] is a δ function [3]. On the other hand, a Fock state, or number states $|N\rangle$, $N = 1,2,3,\ldots$, are at the other extreme in that they are the most nonclassical of field states, having highly sub-Poissonian (or amplitude squeezed) photon-number statistics. The Wigner functions of such states are non-Gaussian, oscillatory, and take on negative values in phase space. The corresponding P functions of the number states are highly singular in that they are given as the $2N$th-order derivative of a δ function.

Optical interferometry with classical-like light beams only, i.e., with coherent light in the state $|\alpha\rangle$ as one input with the other in the vacuum $|0\rangle$, is known to be limited in sensitivity for phase-shift measurements to the standard quantum limit, or shot-noise limit, optimally given by $\Delta\varphi_{\rm SQL} = 1/\sqrt{\bar{n}}$, where $\bar{n} = |\alpha|^2$ is the average number of photons passing through the interferometer [4]. The sensitivity of the interferometer can be enhanced by increasing the intensity of the light, that is, increasing $\bar{n}$. However, this leads to an increase in radiation pressure fluctuations on the interferometer mirrors, thus, ultimately degrading its sensitivity. A possible way around this problem was proposed by Caves [5] who suggested that a form of nonclassical light, namely, a squeezed vacuum (SV) state, be injected into the previously unused port of the first beam splitter of the interferometer along with coherent light as usual. The mixing of coherent and squeezed light at the first beam splitter results in the increase in the sensitivity of the interferometer to $\Delta\varphi = e^{-r}/\sqrt{\bar{n}}$, where $r \geqslant 0$ is the so-called squeezing parameter and $\bar{n}$ still refers to the average photon number of the input coherent state to a good approximation. The measurement scheme for coherent states alone or for coherent states mixed with squeezed vacuum states is the subtraction of the output photocurrents of the second beam splitter, this being the standard approach for the interferometric measurement of phase shifts.

For linear phase shifts, the ultimate level of sensitivity allowed by quantum mechanics is given by the so-called Heisenberg limit $\Delta\varphi_{\rm HL} = 1/\bar{n}$, a reduction in noise over the standard quantum limit by a factor of $1/\sqrt{\bar{n}}$ [6]. There has been much discussion in the literature on the use of so-called NOON states [7] in order to reach this limit, these states having the form $(|N\rangle_a|0\rangle_b + e^{i\Phi_N}|0\rangle_a|N\rangle_b)/\sqrt{2}$, where Φ_N is a phase that may depend on N. Such states cannot be produced with an ordinary beam splitter; some kind of nonlinear process is required to generate them in lieu of the first beam splitter of the interferometer, and one still requires a number state of high photon number N. But with the appropriate observable, which turns out to be the photon-number parity operator of just one of the output beams of the interferometer [8], Heisenberg-limited sensitivity, in this case $\Delta\varphi = 1/N$,can be attained. The use of parity measurements also leads to superresolution. That is, with $\hat{\Pi}$ denoting the parity operator of the relevant output field mode, then $\langle\hat{\Pi}\rangle = \cos(N\varphi)$, which has oscillations in φ that are N times "faster" than for the case of one photon or for interferometry with a coherent state. Oscillations with $N\varphi$ are said to be super-resolved. The necessity of generating number states can be overcome by instead using entangled coherent states of the (un-normalized) form $|\alpha\rangle_a|0\rangle_b + |0\rangle_a|\beta\rangle_b$, where $|\alpha| = |\beta|$, which leads to $\Delta\varphi = 1/\bar{n}$ with $\bar{n} = |\alpha|^2$.

Yet another approach is to use an ordinary interferometer, i.e., one requiring no nonlinear elements as part of the interferometer, with input twin-Fock states $|N\rangle_a|N\rangle_b$ falling on the first beam splitter [9]. With parity measurements on one of the output beams, we obtain asymptotically, in the limit of large N, $\Delta\varphi = 1/(2N)$ [10], which is the Heisenberg limit for this input state, there being $2N$ photons passing though the interferometer. Super-resolved interference fringes in the average of the parity operator are also obtained.

This scheme also has a problem, this having to do with reliably presenting Fock states of equal photon number simultaneously on opposite sides of the first beam splitter. Thus, superpositions of twin-Fock states have been considered. Anisimov *et al.* [11] have studied the use of two-mode squeezed vacuum states, whereas, Gerry and Mimih [12] have studied the use of pair coherent states [13]. Both states yield Heisenberg-limited phase uncertainties and, in fact, the former yield phase uncertainties slightly below the Heisenberg limit for small average photon numbers, whereas, the latter yield phase uncertainties that are very similar to those obtained from the pair coherent states. The initial photon-number distributions of the two-mode squeezed vacuum and pair coherent states are very different. The distribution for the former is super-Poissonian and peaks at the two-mode vacuum state (it is a thermal-like distribution), whereas, the distribution for the latter is sub-Poissonian and peaks around some twin-Fock state $|N\rangle_a|N\rangle_b$ for $\bar{N} \approx N \gg 0, \bar{N}$ being the average photon number in one of the modes.

In all these cases leading to Heisenberg-limited sensitivity, there is a characteristic form of the joint photon-number distribution prior to the final beam splitter and subsequent parity measurement, which is that the photon-number states along the margins are more highly populated than those of the interior. This is obviously true for the NOON states and for the maximally entangled coherent states where the only populated states are exactly along the margins. For the twin-Fock states and their superpositions, after the first beam splitter, the states along the margins are again highly populated, although there is a low plateau of interior states also populated. The point here is that, because of quantum superposition, there is considerable uncertainty in the location of the bulk of the photons. For the NOON state, to take an extreme case, the uncertainty in the number of photons in one of the modes is $\Delta N = N$ (all or none), and by using the heuristic number-phase uncertainty relation $\Delta N\, \Delta\varphi \approx 1$, we obtain $\Delta\varphi \approx 1/N$, the Heisenberg limit.

Some years ago, Ou [14] studied the multiparticle quantum interferences arising in a lossless 50 : 50 beam splitter with N photons (say mode a) as one of the inputs and a single photon at the other (mode b), i.e., with input state $|N\rangle_a|1\rangle_b$. The single photon was shown to have a dramatic effect on the joint photon-number distribution of the state of the photon beams emerging from the beam splitter. For the input state $|N\rangle_a|0\rangle_b$, the joint distribution of the output state is a binomial (Bernoulli) distribution of the N photons over the two output modes. But with the single-photon input, the output distribution, due to multiparticle quantum interference, has a cancellation right in the center of the original binomial distribution. The interference also has the effect of "pushing" the nonzero elements of the distribution over toward the margins. A similar thing happens with input state $|\alpha\rangle_a|1\rangle_b$ where the $N-$photon input state $|N\rangle_a$ is replaced by a coherent state $|\alpha\rangle_a$ [15]. With only a coherent state and a vacuum state $|\alpha\rangle_a|0\rangle_b$ as inputs, the output state of a beam splitter is a product of coherent states, and thus, the joint photon-number distribution is a double Poisson distribution. But with input state $|\alpha\rangle_a|1\rangle_b$, we once again obtain a dramatic change in the distribution, it now having, as before, a central interference fringe with the bulk of the population distribution migrating along the borders. It is the rearrangement of the output joint photon-number distribution, in light of the above remarks on phase and number uncertainties, that has led us to consider such input states in the context of subshot quantum optical interferometry.

In this paper, we examine the prospect of performing super-resolved and supersensitive (i.e., Heisenberg-limited) interferometric measurements with a Mach-Zehnder interferometer (MZI) for input states $|\alpha\rangle_a|N\rangle_b$, $N = 1,2,\ldots$, where it should be noted that we have extended the input number states of the b mode to more than one photon. The multiphoton quantum-interference effects resulting from the mixing of N-photon-number states with coherent states at a beam splitter have not been explored to our knowledge. It turns out that, by mixing photon-number states of increasing photon number N along with coherent states, we obtain both increasing sensitivity (sensitivity beyond the standard quantum limit) approaching the Heisenberg limit and increasing resolution. Motivated by our results from mixing coherent states with number states, we then consider the mixing of coherent states with squeezed vacuum and squeezed one-photon states where the latter can be obtained by photon subtraction from the former. The occupation probabilities of these states are heavily weighted for the low photon-number states. We show that mixing coherent light with squeezed one-photon states leads to improved sensitivity over that obtained by mixing coherent light with squeezed vacuum states.

The paper is organized as follows: In Sec. II, we discuss the mixing of coherent states and number states at a 50 : 50 beam splitter and examine the resulting joint photon-number probability distributions. In Sec. III, we discuss the application of the states to phase-shift detection in interferometry, and in Sec. IV, we extend our considerations to the mixing of squeezed vacuum and squeezed one-photon states. We conclude the paper with some general remarks in Sec. V.

II. MIXING COHERENT AND NUMBER STATES AT A BEAM SPLITTER

We take as our input state to the MZI $|\text{in}\rangle = |\alpha\rangle_a|N\rangle_b$ as indicated in Fig. 1. We can describe the action of a beam splitter as a rotation [16,17] by using the well-known Schwinger realization of the su(2) algebra, $[\hat{J}_i, \hat{J}_j] = i\varepsilon_{ijk}\hat{J}_k$, the $\hat{J}_i (i = 1-3)$ being angular momentum operators, written in terms of two sets of Bose operators as

$$\begin{aligned} \hat{J}_1 &= \frac{1}{2}(\hat{a}^\dagger\hat{b} + \hat{a}\hat{b}^\dagger), \quad \hat{J}_2 = \frac{1}{2i}(\hat{a}^\dagger\hat{b} - \hat{a}\hat{b}^\dagger), \\ \hat{J}_3 &= \frac{1}{2}(\hat{a}^\dagger\hat{a} - \hat{b}^\dagger\hat{b}), \quad \hat{J}_0 = \frac{1}{2}(\hat{a}^\dagger\hat{a} + \hat{b}^\dagger\hat{b}), \end{aligned} \tag{1}$$

where $\hat{J}_0$ is a Casimir operator that commutes with all the others: $[\hat{J}_0, \hat{J}_i] = 0$. The usual angular momentum states $|j,m\rangle$,

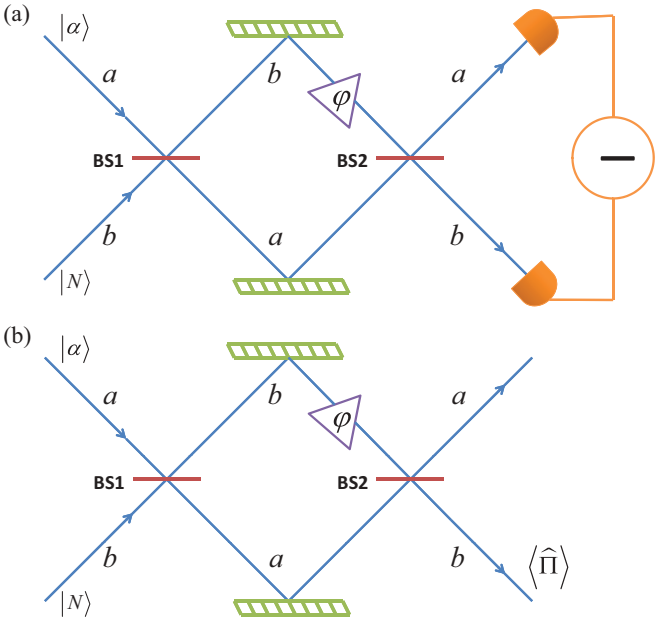

FIG. 1. (Color online) A Mach-Zehnder interferometer with input coherent and number states where φ is the relative phase shift between the two arms where (a) represents the usual detection scheme wherein the output beam photocurrents are subtracted and (b) represents the detection scheme where photon-number parity measurements are performed on just one of the output beams.

which satisfy the eigenvalue relations $\hat{J}_0|j,m\rangle = j|j,m\rangle$ and $\hat{J}_3|j,m\rangle = m|j,m\rangle$, are equivalent to the two-mode product number states $|s\rangle_a|t\rangle_b$ for $j = (s+t)/2$, $m = (s-t)/2$ so that we can write our input state in terms of the angular momentum states as

$$|\text{in}\rangle = |\alpha\rangle_a|N\rangle_b = \exp(-|\alpha|^2/2) \times \sum_{j=N/2,(N+1)/2,(N+2)/2,\ldots}^{\infty} \frac{\alpha^{2j-N}}{\sqrt{(2j-N)!}}|j,j-N\rangle, \quad (2)$$

where the summation over j includes all the half-odd integers.

As shown by Yurke *et al.* [16], the input state $|\text{in}\rangle$ of the MZI is related to the output state $|\text{out}\rangle$ according to

$$|\text{out}\rangle = e^{i(\pi/2)\hat{J}_1}e^{-i\varphi\hat{J}_3}e^{-i(\pi/2)\hat{J}_1}|\text{in}\rangle, \quad (3)$$

where the factors $\exp(\pm i\frac{\pi}{2}\hat{J}_1)$ represent the actions of the 50:50 beam splitters and where the factor $\exp(-i\varphi\hat{J}_3)$ represents the relative phase shifter between the two arms, the relative phase shift being φ.

This set of operators constitutes a particular choice of beam-splitter types, these types defined by the phase shift picked up by the reflected beam. Equivalently, we can write, for the output state,

$$|\text{out}\rangle = e^{-i\varphi\hat{J}_2}|\text{in}\rangle, \quad (4)$$

where we have used the relation $\exp(i\pi\hat{J}_1/2)\hat{J}_3 \times \exp(-i\pi\hat{J}_1/2) = \hat{J}_2$.

For the input state given above, the output state of the first beam splitter is

$$|\text{out,BS1}\rangle = \exp\left(-i\frac{\pi}{2}\hat{J}_1\right)|\text{in}\rangle = e^{-|\alpha|^2/2}\sum_{n=0}^{\infty}\sum_{k=0}^{n}\sum_{q=0}^{N}(-i)^{n-k+N-q} \times \frac{\alpha^n}{n!\sqrt{N!}}2^{-(n+N)/2}\sqrt{(N-q+k)!(n-k+q)!} \times \binom{n}{k}\binom{N}{q}|N-q+k\rangle_a|n-k+q\rangle_b. \quad (5)$$

The probability of detecting m_a photons in mode a and m_b in mode b for a given N is given by

$$P(m_a,m_b|N) = |\langle m_a|\langle m_b|\text{out,BS1}\rangle|^2 = e^{-|\alpha|^2}\frac{|\alpha|^{2(m_a+m_b-N)}m_a!m_b!}{2^{m_a+m_b}[(m_a+m_b-N)!]^2N!} \times \left|\sum_{q=0}^{N} i^{2q}\binom{N}{q}\binom{m_a+m_b-N}{m_a-N+q}\right|^2. \quad (6)$$

For the special cases of $N = 0,1,2,$ and 3, we have

$$P(m_a,m_b|0) = e^{-|\alpha|^2}\frac{|\alpha|^{2(m_a+m_b)}}{2^{m_a+m_b}m_a!m_b!}, \quad (7)$$

$$P(m_a,m_b|1) = e^{-|\alpha|^2}\frac{|\alpha|^{2(m_a+m_b-1)}}{2^{m_a+m_b}m_a!m_b!}(m_a-m_b)^2, \quad (8)$$

$$P(m_a,m_b|2) = e^{-|\alpha|^2}\frac{|\alpha|^{2(m_a+m_b-2)}}{2^{m_a+m_b}m_a!m_b!} \times \left[m_a^2+m_b(m_b-1)+m_a(2m_b+1)\right]^2, \quad (9)$$

and

$$P(m_a,m_b|3) = e^{-|\alpha|^2}\frac{|\alpha|^{2(m_a+m_b-3)}}{2^{m_a+m_b}m_a!m_b!} \times \frac{1}{6}[m_a(m_a-1)(m_a-2)-3m_a(m_a-1)m_b + 3m_am_b(m_b-1)-m_b(m_b-1)(m_b-2)]^2. \quad (10)$$

In Fig. 2, we plot $P(m_a,m_b|N)$ versus m_a and m_b for $|\alpha| = 3$ and for $N = 0,1,2,$ and 3. For $N = 0$, we obtain the expected joint photon-number distribution for input coherent and vacuum states $|\alpha\rangle_a|0\rangle_b$ to the beam splitter, which results, for our choice of beam-splitter type, in the output state $|\alpha/\sqrt{2}\rangle_a|-i\alpha/\sqrt{2}\rangle_b$ the joint photon-number distribution for which is

$$P(m_a,m_b|0) = |_a\langle m_a|\alpha/\sqrt{2}\rangle_{ab}\langle m_b|-i\alpha/\sqrt{2}\rangle_b|^2 = \exp(-|\alpha|^2)\frac{|\alpha/\sqrt{2}|^{2(m_a+m_b)}}{m_a!m_b!}, \quad (11)$$

in agreement with Eq. (7). This is, of course, a unimodal distribution, a composite of Poisson distributions of each of the output coherent states, and is centered near $\bar{n}_a = \bar{n}_b = |\alpha|^2/2$. As is well known, no entanglement is generated in this case. Now, for $N = 1$, we see that the distribution is bimodal. In fact, we can see from Eq. (8) that $P(m,m|1) = 0$ for all m is the

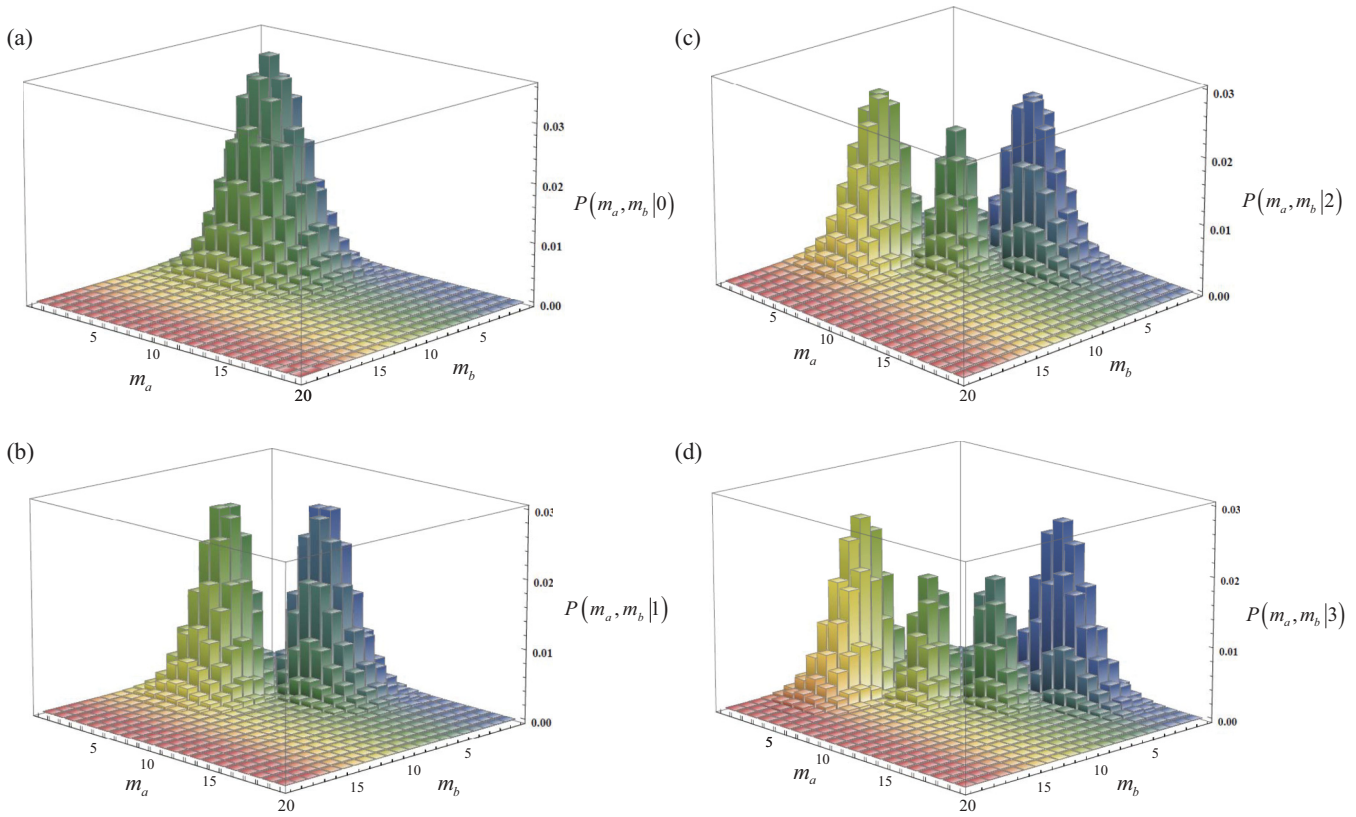

FIG. 2. (Color online) For $\alpha = 3$, (a) the joint photon number distribution $P(m_a,m_b|0)$ plotted against m_a and m_b, (b) for $P(m_a,m_b|1)$, (c) for $P(m_a,m_b|2)$, and (d) for $P(m_a,m_b|3)$.

result of destructive quantum interference. This is a striking result in that $|\alpha|^2$ can be arbitrarily large, yet the appearance of just one photon at the other beam-splitter input dramatically alters the distribution obtained with $N = 0$, bifurcating it into a bimodal distribution. This is interesting in the context of interferometry because the joint photon-number distribution for the NOON state $(|N\rangle_a|0\rangle_b + e^{i\Phi_N}|0\rangle_a|N\rangle_b)/\sqrt{2}$ is also bimodal, although it is nonzero only along the borders (i.e., along the lines $m_a = 0$ and $m_b = 0$). For $N = 2$, we obtain a trimodal distribution. Unlike the case for $N = 1$, we do not have lines of zeros (destructive quantum interference) separating the modes of the distribution, but we do have two lines that *contain* zeros, these being, from Eq. (9), roots of

$$m_a^2 + m_b(m_b - 1) + m_a(2m_b + 1) = 0. \tag{12}$$

The roots of this equation fall along two lines, but there is a not a "continuous" line of zeros. For the case with $N = 3$, we obtain a quadramodal distribution with separations along the lines obtained from the roots of Eq. (10),

$$m_a(m_a - 1)(m_a - 2) - 3m_a(m_a - 1)m_b + 3m_am_b(m_b - 1) - m_b(m_b - 1)(m_b - 2) = 0. \tag{13}$$

The case for which $m_a = m_b = m$ is a solution, e.g., $P(m,m|3) = 0$ for all m. There are other solutions, but these do not form a line of contiguous zeros. Continuing in this way, it is evident that, for a given N, we obtain an $(N + 1)$-modal distribution. For all cases where N is odd, we find that $P(m,m|N_{\rm odd}) = 0$ for all m.

We note also that, with increasing photon number N, the distributions become rearranged symmetrically on an "antidiagonal" in the m_a, m_b plane where the modes (peaks) along the edges are the highest. These are reminiscent of the kinds of distributions that appear upon mixing twin-Fock states by a 50 : 50 beam splitter [10] where the output state is what has been called the arcsine states [17] also known at the "bat states" because of the shape of their joint photon-number distribution across the antidiagonal [18]. As mentioned in the Introduction, it has long been known that twin-Fock states, fed through a Mach-Zehnder interferometer, lead to sub-shot-noise sensitivity measurements of phase shifts. The similarity of the joint distributions obtained upon the mixing of coherent and number states and the mixing of twin-Fock states at a beam splitter suggest that the former should also yield sub-shot-noise phase-shift measurements, which we discuss in the next section.

III. PHASE-SHIFT DETECTION

A. Subtraction of photocurrents

The usual way to obtain information on the relative phase shift φ is to subtract the outputs (the photocurrents) of the second beam splitter as indicated in Fig. 1(a) to obtain the signal $S = \langle(\hat{a}^\dagger\hat{a} - \hat{b}^\dagger\hat{b})_{\rm out}\rangle = 2\langle\hat{J}_{3\,\rm out}\rangle$ where

$$\hat{J}_{3\,\rm out} = e^{i\varphi\hat{J}_2}\hat{J}_3e^{-i\varphi\hat{J}_2} = \hat{J}_3\cos\varphi - \hat{J}_1\sin\varphi. \tag{14}$$

Taking the expectation value of $\hat{J}_{3\,\rm out}$ with respect to $|{\rm in}\rangle = |\alpha\rangle_a|N\rangle_b$, we easily find that $S = (|\alpha|^2 - N)\cos\varphi$.

Using the error propagation calculus, we may determine the uncertainty in estimating the phase shift or the sensitivity of this measurement scheme, according to

$$\Delta\varphi = \Delta J_{3\,\mathrm{out}} \Big/ \left| \frac{\partial \langle \hat{J}_{3\,\mathrm{out}} \rangle}{\partial \varphi} \right|, \tag{15}$$

where $\Delta J_{3\,\mathrm{out}} = \langle \hat{J}^2_{3\,\mathrm{out}} \rangle - \langle \hat{J}_{3\,\mathrm{out}} \rangle^2$. We find that

$$\Delta\varphi = \frac{\sqrt{|\alpha|^2 + N(1+2|\alpha|^2)\sin^2\varphi}}{|(|\alpha|^2 - N)\sin\varphi|}. \tag{16}$$

If $N = 0$, we obtain $\Delta\varphi = 1/\sqrt{\bar{n}|\sin\varphi|}$, where $\bar{n} = |\alpha|^2$, which is the usual result for a coherent state input to the MZI. We notice that the sensitivity depends on the phase shift itself and that the optimal uncertainty is for $\varphi = \pi/2$, which yields the standard quantum limit $\Delta\varphi_{\mathrm{SQL}} = 1/\sqrt{\bar{n}}$. By inserting a quarter-wave plate in the upper arm of the interferometer, one can shift the phase by $\pi/2$ so that, for the general case, we now have

$$\Delta\varphi = \frac{\sqrt{|\alpha|^2 + N(1+2|\alpha|^2)\cos^2\varphi}}{|(|\alpha|^2 - N)\cos\varphi|}, \tag{17}$$

and, for $N = 0$, we have $\Delta\varphi = 1/\sqrt{\bar{n}|\cos\varphi|}$, which goes over to the standard quantum limit in the limit of small phase shift. Thus, with this measure for the phase (i.e., the measurement of the quantity $\hat{J}_3$ at the output of the MZI), for fixed $|\alpha|$, the optimal noise reduction achievable is the standard quantum limit and occurs only for the case when $N = 0$. For other values of N, the noise level rises to above the standard quantum limit. Note that, if the fields are nearly of the same average photon number, i.e., if $|\alpha|^2 \simeq N$, the noise level becomes very high.

B. Photon-number parity measurements

As discussed in the Introduction, an alternative method for detecting the phase shift is through the measurement of photon-number parity on just one of the output beams of the MZI [8] as indicated in Fig. 1(b). We choose this to be the b beam for which the parity operator can be written as

$$\hat{\Pi}_b = (-1)^{\hat{b}^\dagger \hat{b}} = e^{i\pi \hat{b}^\dagger \hat{b}} = e^{i\pi(\hat{J}_0 - \hat{J}_3)}. \tag{18}$$

The expectation value of this operator with respect to the output state is

$$\langle \hat{\Pi}_b(\varphi) \rangle = \langle \mathrm{out}|\hat{\Pi}_b|\mathrm{out}\rangle = \langle \mathrm{in}|e^{i\varphi\hat{J}_2} e^{i\pi(\hat{J}_0 - \hat{J}_3)} e^{-i\varphi\hat{J}_2}|\mathrm{in}\rangle. \tag{19}$$

Writing an arbitrary input state in terms of the angular momentum states $|j,m\rangle$ as

$$|\mathrm{in}\rangle = \sum_{j=0}^{\infty} \sum_{m=-j}^{j} C_{jm} |j,m\rangle, \tag{20}$$

where the sum over j includes the half-odd integers, we can obtain the general result,

$$\langle \hat{\Pi}_b(\varphi) \rangle = \sum_{j=0,1/2,1,3/2,\ldots}^{\infty} \sum_{m=-j}^{j} \sum_{m'=-j}^{j} \sum_{m''=-j}^{j} C^*_{jm'} C_{jm} e^{i\pi(j-m'')} \times d^j_{m',m''}(-\varphi) d^j_{m'',m}(\varphi), \tag{21}$$

where the $d^j_{m',m}(\beta) = \langle j,m'|e^{-i\beta\hat{J}_2}|j,m\rangle$ [19]. For our input states of Eq. (2), we have the coefficients,

$$C_{jm} = \exp(-|\alpha|^2/2) \frac{\alpha^{2j-N}}{\sqrt{(2j-N)!}} \delta_{m,j-N}, \qquad j = \frac{N}{2}, \frac{N+1}{2}, \frac{N+2}{2}, \ldots, \tag{22}$$

so that, after some manipulations, we obtain

$$\langle \hat{\Pi}_b(\varphi) \rangle_N = (-1)^N \exp(-|\alpha|^2) \times \sum_{j=N/2,(N+1)/2(N+2)/2,\ldots}^{\infty} \frac{|\alpha|^{2(2j-N)}}{(2j-N)!} d^j_{j-N,j-N}(2\varphi), \tag{23}$$

or, using the expression for the d functions found in Rose [19], we have

$$\langle \hat{\Pi}_b(\varphi) \rangle_N = (-1)^N \exp(-|\alpha|^2) \times \sum_{j=N/2,(N+1),2,(N+2)/2,\ldots}^{\infty} \frac{|\alpha|^{2(2j-N)}}{(2j-N)!} \times [\cos\varphi]^{2j} {}_2F_1(-N, -2j+N, 1; -\tan^2\varphi), \tag{24}$$

where ${}_2F_1(a,b,c;x)$ is the hypergeometric function.

First, we consider the special case $N = 0$ for which we can obtain the simple form

$$\langle \hat{\Pi}_b(\varphi) \rangle_0 = \exp[-\bar{n}(1 - \cos\varphi)], \tag{25}$$

where $\bar{n} = |\alpha|^2$. This is just the result obtained by Chiruvelli and Lee [20] and discussed by Gao *et al.* [21] in connection with an application of parity measurements to the problem of the quantum laser radar. Note that, for small angles $\varphi \to 0$, we obtain a signal peaking with $\langle \hat{\Pi}_b(0) \rangle_0 = 1$ but which becomes narrower around $\varphi = 0$ for increasing $\bar{n}$. The signal is not super-resolved in the usual sense of having oscillations frequencies scaling as $M\varphi$ for integer $M > 1$. However, compared with the corresponding result for the output subtraction method $S/\bar{n} = \cos\varphi$, we can see the signal for the parity measurement $\exp[-\bar{n}(1 - \cos\varphi)]$ is much narrower, and it is in this sense that Gao *et al.* [21] interpret the parity result as being super-resolved.

Now, we turn to the general cases for which $N > 1$ for which we plot $\langle \hat{\Pi}_b(\varphi) \rangle_N$ against φ in Fig. 3 for various $|\alpha|^2$. Note that, in the limit $\varphi \to 0$, we have, from Eq. (24), that

$$\langle \hat{\Pi}_b(\varphi = 0) \rangle_N = (-1)^N \exp(-|\alpha|^2) \times \sum_{j=N/2,(N+1)/2,(N+2)/2,\ldots}^{\infty} \frac{|\alpha|^{2(2j-N)}}{(2j-N)!} = (-1)^N, \tag{26}$$

and, thus, the expectation value of the parity operator for the output b mode at $\varphi = 0$ exactly reflects the parity of N. But we also get oscillations in the signal with φ (interference fringes) of the type expected in the usual sense of super-resolution, and furthermore, we notice that the central peak or valley at $\varphi = 0$ narrows for increasing N. Thus, the injection of

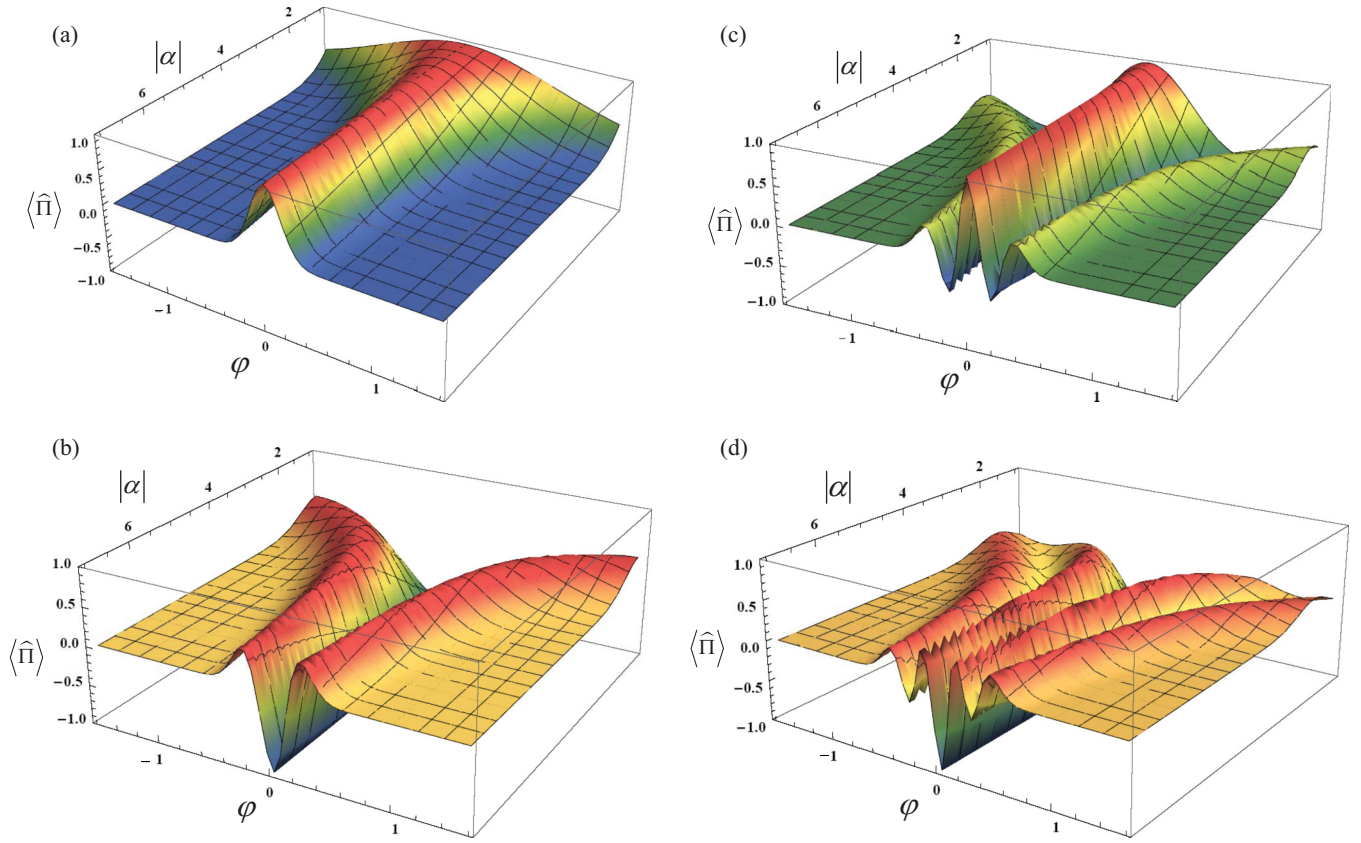

FIG. 3. (Color online) Expectation value of the parity operator for the output b beam plotted against the phase shift φ and $|\alpha|$ for (a) $N = 0$, (b) $N = 1$, (c) $N = 2$, and (d) $N = 3$.

photon-number states along with coherent states into the MZI apparently leads to enhanced super-resolution because of the narrowing of the central peak or valley and in the increase in the number of oscillations in the signal with changing φ.

Finally, we consider the effects on noise reduction with parity operator measurements. From the error propagation calculus for the parity observable, we have

$$\Delta\varphi = \frac{\Delta\Pi_b}{|\partial\langle\hat{\Pi}_b(\varphi)\rangle/\partial\varphi|} = \frac{\sqrt{1-\langle\hat{\Pi}_b(\varphi)\rangle^2}}{|\partial\langle\hat{\Pi}_b(\varphi)\rangle/\partial\varphi|}, \tag{27}$$

where $\Delta\hat{\Pi}_b = \sqrt{\langle\hat{\Pi}_b^2(\varphi)\rangle - \langle\hat{\Pi}_b(\varphi)\rangle^2}$ and where $\langle\hat{\Pi}_b^2(\varphi)\rangle = 1$. In Fig. 4, we plot $\Delta\varphi$ against the total average photon number $|\alpha|^2 + N$ for $N = 0,1,2,$ and 3 in the limit $\varphi \to 0$ where, for computation reasons, we set $\varphi = 10^{-4}$.Included in each graph are the corresponding standard quantum limit $\Delta\varphi_{\mathrm{SQL}} = 1/\sqrt{|\alpha|^2 + N}$ and the Heisenberg limit $\Delta\varphi_{\mathrm{HL}} = 1/(|\alpha|^2 + N)$. It is evident that mixing coherent states with a Fock state of N photons allows for sub-shot-noise limit noise reduction in the parity-based measurement scheme of detecting phase shifts. The effect is most pronounced for intermediate values of $|\alpha|^2 + N$ where, even for $N = 1$, we see a remarkable reduction in the noise level. It is clear that, overall, the noise reduction approaches the Heisenberg limit for increasing N.

The minimal phase uncertainty obtainable for a given state is found by the quantum Cramér-Rao bound [22],

$$\Delta\varphi_{\mathrm{min}} = 1/\sqrt{F_Q}, \tag{28}$$

where F_Q is the quantum Fisher information for an MZI. F_Q is four times the variance of the operator $\hat{J}_3$ that generates the accumulated phase shift between the arms of the interferometer [11,13], this being the factor $\exp(-i\varphi\hat{J}_3)$ in Eq. (3). That is, $F_Q = 4\Delta\hat{J}_3$. For our input states $|\alpha\rangle_a|N\rangle_b$, we find that

$$\Delta\varphi_{\mathrm{min}} = \frac{1}{2\sqrt{|\alpha|^2 + N(1+2|\alpha|^2)\cos\varphi}}. \tag{29}$$

It turns out that the phase-shift uncertainties obtained with this result in the limit $\varphi \to 0$, the dots in Fig. 4, exactly agree with those obtained by the parity operator method, a result that is in agreement with those of Refs. [11,23], which also show that the measurement of the photon-number parity operator realizes the Cramér-Rao bound.

IV. MIXING COHERENT STATES WITH SQUEEZED VACUUM STATES AND SQUEEZED ONE-PHOTON STATES

So far, we have discussed the effects of mixing coherent states with number states at a beam splitter. For a general superposition of number states in mode b of the form

$$|\psi\rangle_b = \sum_{N=0}^{\infty} C_N|N\rangle_b, \tag{30}$$

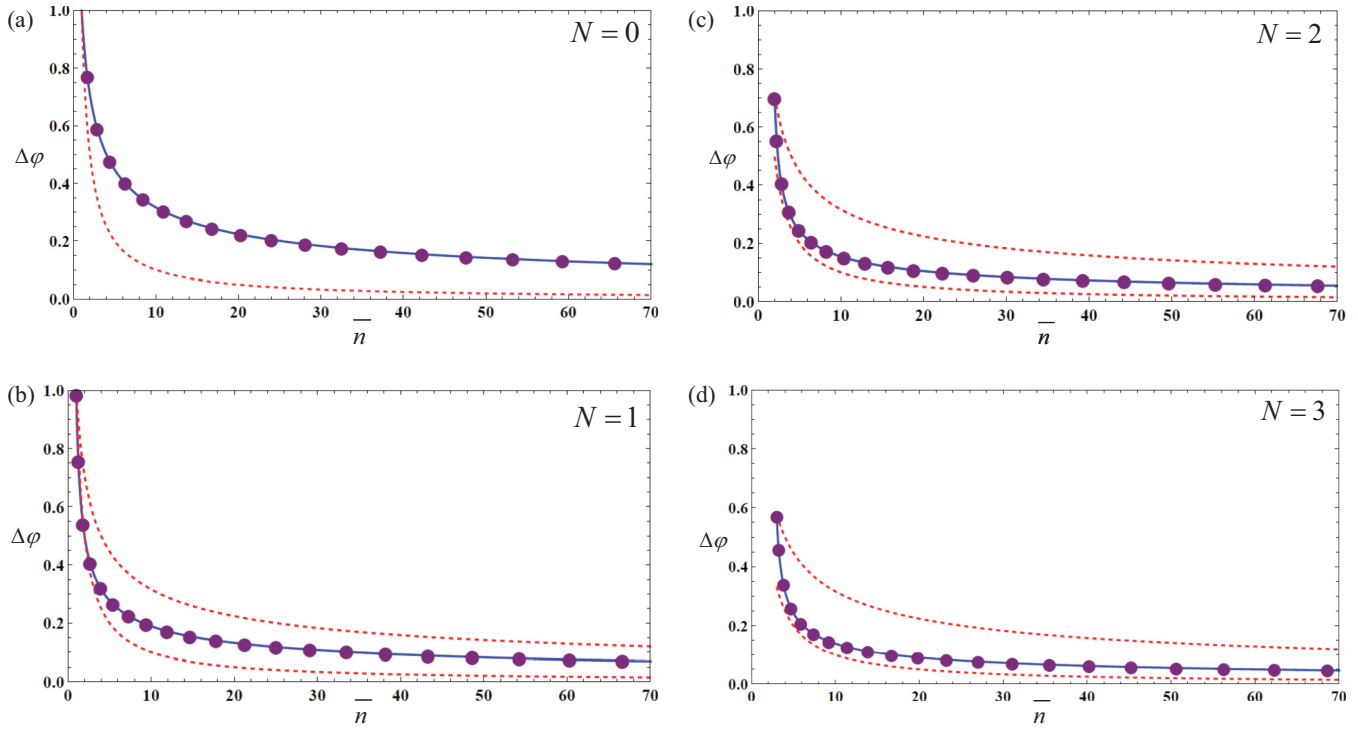

FIG. 4. (Color online) The phase uncertainty $\Delta\varphi$ versus the total average photon number $\bar{n} = |\alpha|^2 + N$ with the choice $\varphi = 10^{-4}$ rad for (a) $N = 0$, (b) $N = 1$, (c) $N = 2$, and (d) $N = 3$. The upper dashed line represents the corresponding standard quantum limit, and the lower dashed line represents the Heisenberg limit. The dots represent the results obtained for the Cramér-Rao bound given by Eq. (28). We include (a) the case $N = 0$ as a reminder that, when performing parity measurements for input coherent light only, one reaches the standard quantum limit for low values of the phase shift in contrast to what happens using subtraction of photocurrents leading to Eq. (16).

the input state is $|\text{in}\rangle = |\alpha\rangle_a|\psi\rangle_b$. After the first beam splitter, we have

$$\begin{aligned}|\text{out, BS1}\rangle &= e^{-i(\pi/2)J_1}|\text{in}\rangle \\ &= \sum_{N=0}^{\infty}\sum_{n=0}^{\infty}\sum_{k=0}^{n}\sum_{q=0}^{N} C_N e^{-|\alpha|^2/2}(-i)^{n-k+N-q} \\ &\quad\times \frac{\alpha^n}{n!\sqrt{N!}}2^{-(n+N)/2} \\ &\quad\times\sqrt{(N-q+k)!(n-k+q)!}\binom{n}{k}\binom{N}{q} \\ &\quad\times |N-q+k\rangle_a|n-k+q\rangle_b, \end{aligned} \tag{31}$$

The probability of detecting m_a photons in mode a and m_b in mode b is given by

$$\begin{aligned}&P(m_a,m_b|\psi) \\ &= e^{-|\alpha|^2}\frac{m_a!m_b!}{2^{m_a+m_b}}\left|\sum_{N=0}^{\infty}\sum_{q=0}^{N} C_N i^{(2q-N)}\frac{\alpha^{m_a+m_b-N}}{(m_a+m_b-N)!\sqrt{N!}}\right. \\ &\quad\left.\times\binom{N}{q}\binom{m_a+m_b-N}{m_a-N+q}\right|^2. \end{aligned} \tag{32}$$

The corresponding expectation value of the parity operator is given by

$$\langle\hat{\Pi}_b\rangle = \sum_{N=0}^{\infty}|C_N|^2\langle\hat{\Pi}_b\rangle_N. \tag{33}$$

In the paper of Caves [5], coherent states are mixed with single-mode squeezed vacuum states at a beam splitter. A single-mode squeezed number state in the b mode is given by [24,25]

$$|r,M\rangle_b = \hat{S}_b(r)|M\rangle_b, \tag{34}$$

where $\hat{S}_b(r)$ is the squeeze operator given by

$$\hat{S}_b(r) = \exp\left[\frac{1}{2}r(\hat{b}^{\dagger 2} - \hat{b}^2)\right], \tag{35}$$

and where r is the squeeze parameter $0 \leqslant r < \infty$. For the squeezed vacuum state $M = 0$, we have

$$|r,0\rangle_b = \sum_{N=0}^{\infty} C_N|N\rangle_b, \tag{36}$$

where [23]

$$C_N = \begin{cases}(-1)^{N/2}\left[\frac{N!}{2^N[(N/2)!]^2}\frac{\tanh^N r}{\cosh r}\right]^{1/2}, & N \text{ even}, \\ 0, & N \text{ odd}.\end{cases} \tag{37}$$

The average photon number for the squeezed vacuum state is

$$\bar{n} = \sinh^2 r. \tag{38}$$

For the case of the one-photon squeezed state $M = 1$, we have

$$C_N = \begin{cases}0, & N \text{ even}, \\ (-1)^{(N-1)/2}\left[\frac{N!}{2^{N-1}\{[(N-1)/2]!\}^2}\frac{\tanh^{N-1} r}{\cosh^3 r}\right]^{1/2}, & N \text{ odd}.\end{cases} \tag{39}$$

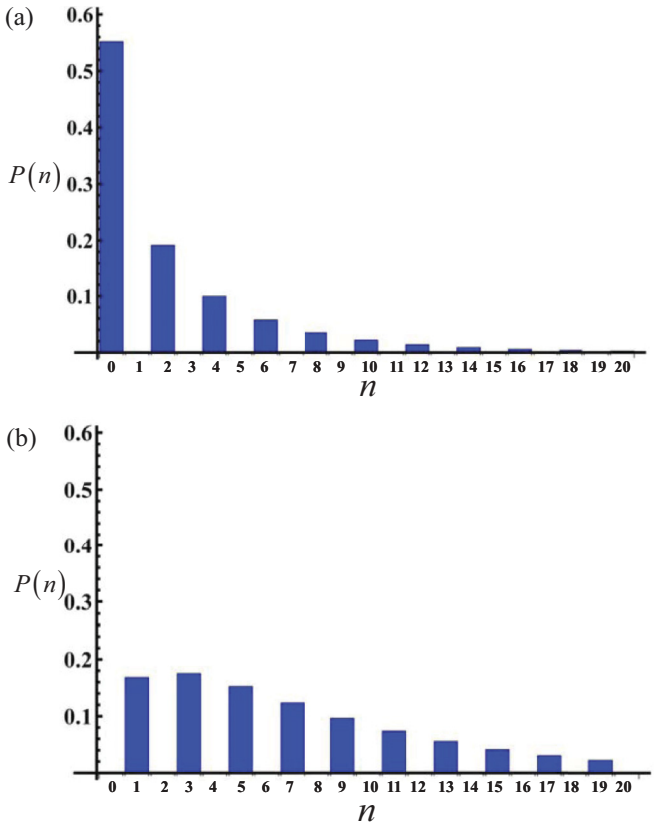

FIG. 5. (Color online) Photon-number probability distributions for (a) the single-mode squeezed vacuum state and (b) the single-mode squeezed one-photon states, both for squeeze parameter $r = 1.2$.

The average photon number for this state is given by [24]

$$\bar{n} = \sinh^2 r + \cosh(2r). \tag{40}$$

The photon-number probability distributions for these states, given by $P_N = |C_N|^2$, are plotted against N in Fig. 5 for squeeze parameter $r = 1.2$. For a given value of r, the average number of photons in the squeezed vacuum and squeezed one-photon states is quite different. For $r = 1.2$, the average number of photons in the squeezed vacuum state is 2.278, whereas for the squeezed one-photon state it is 7.835.

Now, by mixing coherent and squeezed vacuum states at a beam splitter, it is possible to choose field-state parameters such that, after beam splitting, the joint photon-number distribution is symmetrically populated along the borders with essentially no population in the interior. In Fig. 6, we display such a situation for the case where $\alpha = \sqrt{1.2}$ and $r = 0.947$, which corresponds to beams of equal average photon number 1.2. We see that the output state consists of a superposition of NOON states for $N = 2,3,4$, and 5. The α and r parameters used for the above graph are those relevant to a recent experiment performed by Afek *et al.* [26] who, working on a suggestion by Hofmann and Ono [27], have performed an interferometry experiment based on the NOON states contained in the superposition of NOON states (found in the output state of the first beam splitter) in which they obtained high sensitivity and super-resolution in the measurement of phase shifts. The idea of the experiment was to use a setup

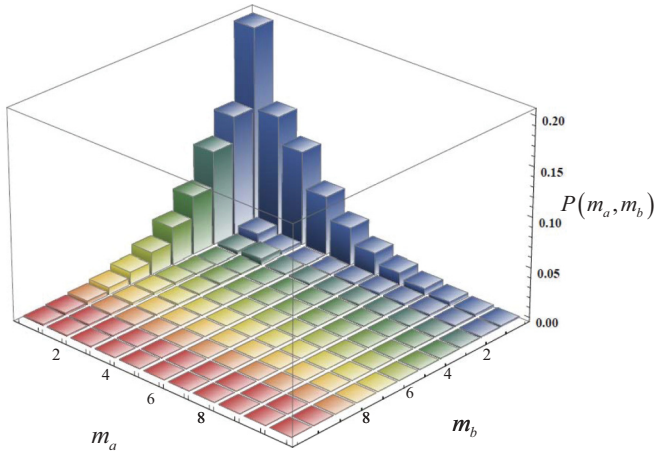

FIG. 6. (Color online) The joint photon-number distribution after beam splitting for equal intensity coherent and squeezed vacuum states corresponding to $\alpha = \sqrt{1.2}$ and $r = 0.947$.

similar to the one pictured in Fig. 1(a) but to count only the coincident counts where the total photon numbers counted added up the selected value of N. In other words, they measured $\langle(\hat{a}^\dagger\hat{a}\hat{b}^\dagger\hat{b})_{\rm out}\rangle$ but retained only the counts where, say, if one detector detects m photons, the other detects $N - m$ and where all other counts, whose total does not add to N, are discarded. This amounts to a projection measurement onto a subspace wherein the photon numbers in the two modes add up to N. In the experiment reported in Ref. [26], the total photon numbers $N = 2{-}5$ were studied, and sub-shot-noise and super-resolved phase-shift measurements were performed. However, it seems to be the case that equal intensity input coherent and squeezed vacuum states yield photon-number distributions of the type shown in Fig. 6 only for relatively low values of $|\alpha|$. For larger values of $|\alpha|$, many states in the plane are populated (see below), and one does not have a superposition of NOON states.

With parity measurements performed on one of the output beams, it is not necessary, or even possible, to restrict oneself to a definite N-photon NOON state, and that can be an advantage. The total number of photons inside the interferometer for this input state is indeterminate, but the Heisenberg limit is approached in terms of the average of the total photon number. Seshadreesan *et al.* [28] have already shown that photon-number parity-measurement-based interferometry reaches the Heisenberg limit if coherent state and squeezed vacuum light of equal intensity are mixed at a 50 : 50 beam splitter.

In the case of the squeezed vacuum state, the vacuum state component itself has the highest probability of occupation, the photon-number distribution being thermal-like apart from the fact that only the even photon-number states are populated. However, for the squeezed one-photon state, the vacuum is not present, and it is the one-photon state itself that dominates the corresponding photon-number probability distribution. It seems reasonable, based on the dramatic improvement to sensitivity obtained by mixing the one-photon state with a coherent state, to suspect that the squeezed one-photon state mixed with coherent light might perform better in interferometry than does mixing coherent light with the squeezed vacuum for the same values of α and r. The total average photon numbers passing

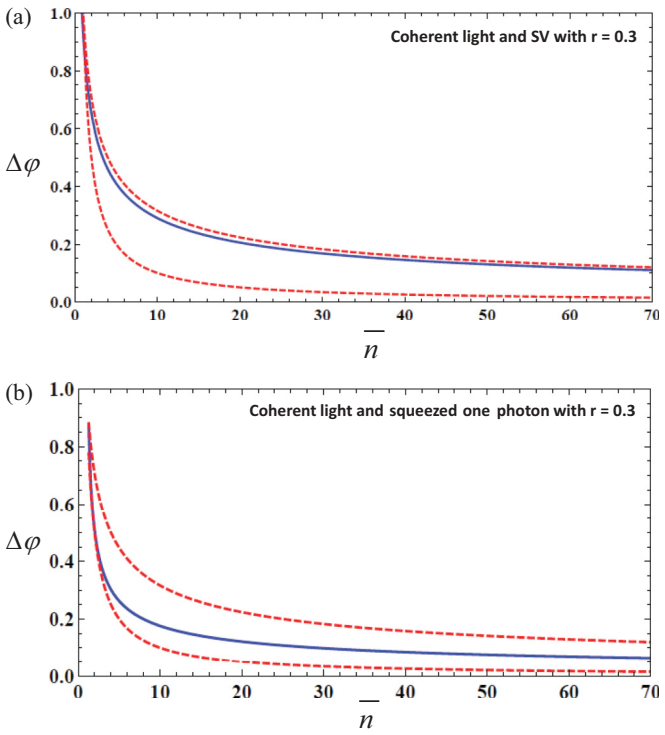

FIG. 7. (Color online) Phase uncertainties against the total average photon number for coherent light mixed with (a) the squeezed vacuum and (b) with squeezed one-photon states for the choice of $r = 0.3$ and for $\varphi = 10^{-4}$.

through the interferometer in these cases is

$$\bar{n} = |\alpha|^2 + \sinh^2 r, \tag{41}$$

and

$$\bar{n} = |\alpha|^2 + \cosh(2r) + \sinh^2 r \tag{42}$$

for the squeezed vacuum and squeezed one-photon states, respectively, mixed with a coherent state. In Fig. 7, we plot the corresponding phase uncertainties against the total average photon number for the mixing of coherent light with the squeezed vacuum [Fig. 7(a)] and squeezed one-photon states [Fig. 7(b)] for the choice $r = 0.3$ where we have taken the phase shift to be $\varphi = 10^{-4}$. We repeat for $r = 0.9$ in Fig. 8. As we expected, the squeezed one-photon state outperforms the squeezed vacuum state, significantly reducing the noise in both examples for a given total average photon number.

An explanation for the improvement in performance by the squeezed one-photon state can be provided by examining the joint photon-number distribution after the first beam splitter. In Fig. 9(a), we plot the joint photon-number probability distribution after the mixing of a coherent state with a squeezed one-photon state for the case of $\alpha = 2$ and $r = 0.9$ where the states are not of equal intensity. The average total photon number for this state is $\bar{n} = 8.161$. In Fig. 9(b), we plot the distribution for the coherent state mixed with a squeezed vacuum state with the same parameters. The average total photon number for this state is $\bar{n} = 5.054$. In the former case, the distribution is bimodal, populated mainly on the borders with Poisson-like distributions on each axis and with peaks near $n_{a,b} = 8.161 = \bar{n}$. This distribution

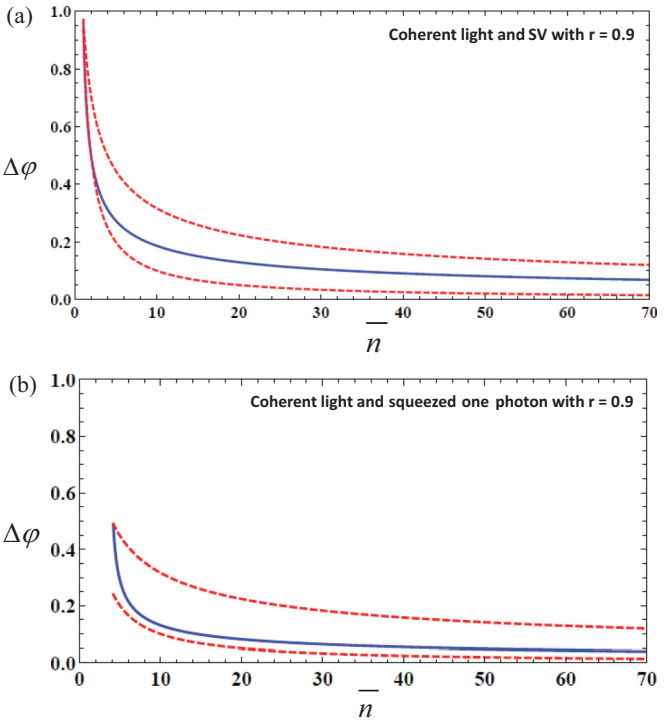

FIG. 8. (Color online) Same as Fig. 7 but for $r = 0.9$.

resembles that of an entangled coherent state of the form $|\beta\rangle_a|0\rangle_b + \exp(i\Phi)|0\rangle_a|\beta e^{i\delta}\rangle_b$, the coherent state analog of the NOON, a superposition of NOON states, and known to be effective in performing Heisenberg-limited interferometry in terms of the average total photon number for small phase shifts [29]. In contrast, the distribution involving the squeezed vacuum has some separation along the borders but also has considerable population on the inside. In Fig. 10, we plot the expectation value of the parity operator for the mixing of coherent states with the squeezed vacuum and squeezed one-photon states. It is evident that the resolution obtained for the latter case is enhanced over that of the former.

It is worth noting that the measurement scheme of Ref. [26] requires photon counting with resolution at the level of a single photon. Photon counts at the same level of resolution can also be used to perform photon-number parity measurements, so no new technology would be required to perform such measurements, at least for photon numbers that are not too high. (On the other hand, quantum nondemolition techniques can be used to measure the parity directly, at least in principle, Ref. [30].)

Lastly, in this section, we point out that there is no need to first supply a one-photon state $|1\rangle$, which would then be subjected to the parametric amplifier that performs the squeezing operation to generate the squeezed one-photon state. Instead, as has been shown by Biswas and Agarwal [31], the state obtained by subtracting a single photon from the squeezed vacuum is identical to the squeezed one-photon state. For completeness, we repeat the demonstration here. The squeezed vacuum and one-photon states are given, respectively, by

$$|r,0\rangle_b = \hat{S}_b(r)|0\rangle_b, \quad |r,1\rangle_b = \hat{S}_b(r)|1\rangle_b. \tag{43}$$

We subtract one photon from the squeezed vacuum state, i.e., perform the operation $\hat{b}|r,0\rangle_b$, which we can write, using

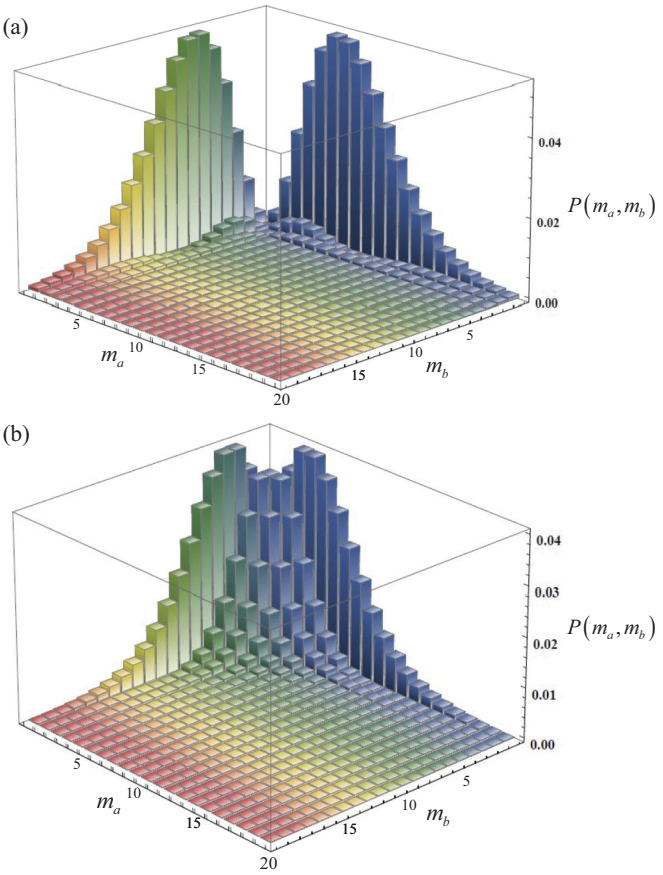

FIG. 9. (Color online) (a) Plot of the joint photon-number probability distribution after the mixing of a coherent state with a squeezed one-photon state for the case of $\alpha = 2$ and $r = 0.9$, and the average total photon number for this state is $\bar{n} = 8.133$. (b) Plot of the distribution for the mixed coherent squeezed vacuum states with the same parameters. The average total photon number for this state is $\bar{n} = 5.026$.

the unitarity of the squeezing operator, as

$$\hat{b}|r,0\rangle_b = \hat{b}\hat{S}_b(r)|0\rangle_b = \hat{S}_b(r)\hat{S}_b^\dagger(r)\hat{b}\hat{S}_b(r)|0\rangle_b. \quad (44)$$

Using the relation,

$$\hat{S}_b^\dagger(r)\hat{b}\hat{S}_b(r) = \hat{b}\ \cosh r + \hat{b}^\dagger \sinh r, \quad (45)$$

we have

$$\hat{b}|r,0\rangle_b = \sinh\ r\hat{S}_b(r)|1\rangle_b, \quad (46)$$

from which it follows that

$$|r,1\rangle_b = \hat{S}_b(r)|1\rangle_b = \frac{1}{\sinh r}\hat{b}|r,0\rangle_b. \quad (47)$$

Photon-subtracted squeezed vacuum states have already been made available in the laboratory [32,33] with up to three photons subtracted.

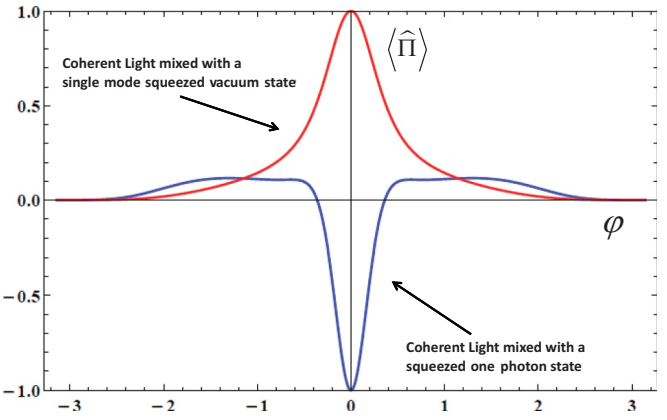

FIG. 10. (Color online) Plot of the expectation value of the output b-mode photon-number parity operator versus φ for mixed coherent, squeezed vacuum, and squeezed one-photon states for $\alpha = 2$ and $r = 0.9$. The total average photon number in the case of the squeezed vacuum state is $\bar{n} = 5.054$ where, for the case of the squeezed one-photon state, it is $\bar{n} = 8.161$. The curve for the latter case is narrower than that for the former indicating an increase in resolution.

V. CONCLUSIONS

In this paper, we have studied the multiphoton interference obtained by mixing coherent states of light $|\alpha\rangle$ with photon-number states $|N\rangle$ of low photon number $N = 1,2,$ and 3 at a 50 : 50 beam splitter and have investigated the prospects of performing quantum optical interferometric measurements with them. When coherent light is mixed with a photon-number state, the resulting multiphoton interference creates joint photon-number probability distributions that are multimodal and symmetric about the diagonal line $n_a = n_b$. The structure of these distributions, the fact that they split into distributions that lead to uncertainty as to the location of the bulk of the photons, is key to the effectiveness of such states for approaching Heisenberg-limited sensitivity in the measurements of phase shifts. The distributions obtained from the mixing of coherent states with number states resembles the kinds of distributions obtained from the mixing of twin-number states at a 50 : 50 beam splitter where the output states are the arcsine states [10] also known as the bat states. With regard to phase-shift measurements, which are performed with the use of photon-number parity detections on one of the output beams, we have noticed a significant improvement over the standard quantum limit obtained with coherent-state mixing with a vacuum state by mixing the coherent light with a single photon. This happens because of the dramatic effect that occurs in this case where the joint Poisson distribution obtained from coherent light alone is bifurcated along the line $m_a = m_b$ as the result of quantum interference with just one photon. To us, this suggested the possibility that the squeezed one-photon state, because the one-photon state itself is the lowest number state therein and has a relatively high probability of occurrence, should be more effective in obtaining substandard quantum limit noise reductions than the squeezed vacuum. This expectation was confirmed. We pointed out that it was not even necessary to squeeze a one-photon state (a difficult task) as one can obtain it identically by subtracting a single photon from a squeezed vacuum state as shown by Biswas and

Agarwal [31]. The possibilities and benefits for using multiple photon-subtracted squeezed states in interferometry is under investigation and will be reported on elsewhere.

ACKNOWLEDGMENT

This research was supported by a grant from PSC-CUNY.

[1] R. J. Glauber, Phys. Rev. **131**, 2766 (1963).
[2] E. C. G. Sudarshan, Phys. Rev. Lett. **10**, 277 (1963).
[3] M. Hillery, Phys. Lett. A **111**, 409 (1985).
[4] See, for example, C. C. Gerry and P. L. Knight, *Introductory Quantum Optics* (Cambridge University Press, Cambridge, UK, 2005), p. 146.
[5] C. M. Caves, Phys. Rev. D **23**, 1693 (1981).
[6] Heisenberg limit.
[7] See J. P. Dowling, Contemp. Phys. **42**, 125 (2008), and references therein.
[8] See C. C. Gerry and J. Mimih, Contemp. Phys. **51**, 497 (2010), and references therein.
[9] M. J. Holland and K. Burnett, Phys. Rev. Lett. **71**, 1355 (1993).
[10] R. A. Campos, C. C. Gerry, and A. Benmoussa, Phys. Rev. A **68**, 023810 (2003).
[11] P. M. Anisimov, G. M. Raterman, S. Chiruvelli, W. N. Plick, S. D. Huver, H. Lee, and J. P. Dowling, Phys. Rev. Lett. **104**, 103602 (2010).
[12] C. C. Gerry and J. Mimih, Phys. Rev. A **82**, 013831 (2010).
[13] G. S. Agarwal, Phys. Rev. Lett. **57**, 827 (1986); J. Opt. Soc. Am. B **5**, 1940 (1988).
[14] Z. Y. Ou, Quantum Semiclass. Opt. **8**, 315 (1996); See also Z. Y. J. Ou, *Multiphoton Quantum Interference* (Springer, New York, 2007), Chap. 10.
[15] A. Kuzmich, D. Manning, L. Mandel, and I. A. Walmsley, J. Mod. Opt. **45**, 2233 (1998).
[16] B. Yurke, S. L. McCall, and J. R. Klauder, Phys. Rev. A **33**, 4033 (1986).
[17] R. A. Campos, B. E. A. Saleh, and M. C. Teich, Phys. Rev. A **40**, 1371 (1989).
[18] See J. Joo, W. J. Munro, and T. P. Spiller, Phys. Rev. Lett. **107**, 083601 (2011); **107**, 219902(E) (2011).
[19] M. E. Rose, *Elementary Theory of Angular Momentum* (Dover, Mineola, NY, 1995), p. 53.
[20] A. Chiruvelli and H. Lee, J. Mod. Opt. **58**, 945 (2011).
[21] Y. Gao, P. M. Anisimov, C. F. Wildfeuer, J. Luine, H. Lee, and J. P. Dowling, J. Opt. Soc. Am. B **27**, A170 (2010).
[22] See S. L. Braunstein and C. M. Caves, Phys. Rev. Lett. **72**, 3439 (1994); S. L. Braunstein, C. M. Caves, and G. J. Milburn, Ann. Phys. (NY) **247**, 135 (1996).
[23] Y. Ben-Aryeh, J. Opt. Soc. Am. B **29**, 2754 (2012).
[24] M. S. Kim, F. A. M. de Oliviera, and P. L. Knight, Phys. Rev. A **40**, 2494 (1989).
[25] L. Albano, D. F. Mundarin, and J. Stephany, J. Opt. B **4**, 352 (2002).
[26] I. Afek, O. Ambar, and Y. Silberberg, Science **328**, 879 (2010).
[27] H. F. Hofmann and T. Ono, Phys. Rev. A **76**, 031806 (2007).
[28] K. P. Seshadreesan, P. M. Anisimov, H. Lee, and J. P. Dowling, New J. Phys. **13**, 083026 (2011).
[29] C. C. Gerry and R. A. Campos, Phys. Rev. A **64**, 063814 (2001); C. C. Gerry, A. Benmoussa, and R. A. Campos, *ibid.* **66**, 013804 (2002).
[30] C. C. Gerry, A. Benmoussa, and R. A. Campos, Phys. Rev. A **72**, 053818 (2005).
[31] A. Biswas and G. S. Agarwal, Phys. Rev. A **78**, 032104 (2007).
[32] A. Ourjoumtsev, R. Tualle-Brouri, J. Laurat, and P. Grangier, Science **312**, 83 (2006).
[33] T. Gerrits, S. Glancy, T. S. Clement, B. Calkins, A. E. Lita, A. J. Miller, A. L. Migdall, S. W. Nam, R. P. Mirin, and E. Knill, Phys. Rev. A **82**, 031802(R) (2010).